Egyptian Informatics Journal (2015) 16, 175–185

Cairo University

Egyptian Informatics Journal

www.elsevier.com/locate/eij
www.sciencedirect.com

ORIGINAL ARTICLE

Data fitting by G^1 rational cubic Bézier curves using harmony search

Najihah Mohamed [a,*], Ahmad Abd Majid [b], Abd Rahni Mt Piah [b]

[a] *Faculty of Industrial Sciences & Technology, Universiti Malaysia Pahang, Lebuhraya Tun Razak, 26300 Kuantan, Pahang, Malaysia*
[b] *School of Mathematical Sciences, Universiti Sains Malaysia, 11800 USM, Pulau Pinang, Malaysia*

Received 3 December 2014; revised 23 March 2015; accepted 14 May 2015
Available online 6 June 2015

KEYWORDS

Rational cubic Bézier;
Data approximation;
Harmony search

Abstract A metaheuristic algorithm, called Harmony Search (HS) is implemented for data fitting by rational cubic Bézier curves. HS is a derivative-free real parameter optimization algorithm, and draws an inspiration from the musical improvisation process of searching for a perfect state of harmony. HS is suitable for multivariate non-linear optimization problem. It is mainly achieved by data fitting using rational cubic Bézier curves with G^1 continuity for every joint of segments of the whole data sets. This approach has significant contributions in making the technique automated. HS is used to optimize positions of middle points and values of the shape parameters. Test outline images and comparative experimental analysis are presented to show effectiveness and robustness of the proposed method. Statistical testing between HS and two other different metaheuristic algorithms is used in the analysis on several outline images. All of the algorithms improvised a near optimal solution but the result that is obtained by the HS is better than the results of the other two algorithms.

1. Introduction

Data fitting is a well-studied area in computer graphics and mathematics which is also a fundamental problem in many fields, such as computer graphics, image processing, shape modelling and data mining. Depending on applications, different types of curves such as parametric curves, implicit curves and subdivision curves are used for fitting. Data fitting is normally divided into two types, approximation and interpolation. Under an approximation-fitting scheme, a curve must pass reasonably close to the data points but is not required to pass through them [12].

Rational Bézier curves are widely used in CAD/CAGD fields, because they have concise and geometrically meaningful presentation and can be deformed easily by moving the control points or modifying weights. Some studies on data fitting using rational Bézier functions, to determine the best conic approximation of a given curve which is based on Hausdorff distance

* Corresponding author.
Peer review under responsibility of Faculty of Computers and Information, Cairo University.

Production and hosting by Elsevier

http://dx.doi.org/10.1016/j.eij.2015.05.001
1110-8665

function [7], approximate rational Bézier curves by Bézier curves through the concept of $C^{(u,v)}$ – continuity [1] and as iteration method for approximation of rational Bézier curves by adjusting control points gradually using the scheme of weighted progressive iteration approximations through a global L_p – error [9]. Recently, a few researchers such as Huang et al. [6] whose derived offset by using cubic Bézier for approximating degree n Bézier with comparing three methods, Hausdorff distance, shifting control and approximation based on L_2 norm in order to find the better approximation. While Yang et al. [21] focused on curves on surfaces which present a parabola approximation method based on the cubic rational Bézier surfaces. This study also used Hausdorff distance between the approximate curve and the exact curve; the approximation is controlled under the user-specified tolerance. Shen et al. [17] proposed a certified approximation as an optimization method to select proper weights in the cubic rational Bézier curve to approximate the given curve. The error of the approximation is controlled by the size of its tetrahedron, which converges to zero by subdividing the curve segments. Stamati and Fudos [20] presented a fast curve approximation method that approximates raw data with cubic rational Bézier curves. The approach combines least squares approximation with continuity constraints to ensure G^1 continuity between neighbouring curves. This study imposed continuity constraints into the least squares optimization process to ensure that the computed control points respect the estimated tangents at the end points.

Meanwhile, a few researchers had used metaheuristic method recently to curve fit outline images or a set of data points such as Sarfraz [18] that used simulated annealing to curve fit extracting outlines of images with a generalized cubic spline, the simulated annealing is used to optimize the shape parameter and another paper [19] also used simulated annealing as the mechanism to globally optimizes the shape parameters in the description of the conic splines but in the case of poor approximation, the insertions of intermediate points are made as long as the desired approximation is achieved. Yahya [16] proposed particle swarm optimization to optimize the control points and weight which were then used in conic equations. While, Gálvez and Iglesias [3] applied PSO to compute an appropriate location of knots as the knots were treated as free variables for B-splines functions.

In this paper, a metaheuristic approach namely, HS is implemented as an approximation tool using rational cubic Bézier curve from given data points. Our algorithm is based on the idea of minimizing least-squares error by Yahya [14] in order to improve positions of two middle control points, C_1, C_2 and values of weights, $w_1 and w_2$ as in Yahya et al. [15]. We use the adjustments adjust its shape and parametric structure so as to construct curves that pass as closely as possible between the data sets smoothly. We also adjust and control points and values of weights until the error of the least squares is minimized. Therefore, the best approximation with minimum least-squares error can be obtained by this technique. The aim of this study was to prove that HS can be used as a method to fit a set of data points via rational cubic Bézier and also as a best method based on its time consuming and guarantee to nearly reach the global optimal solution and locally optimal solution as it has a stoping criteria with the best solution it has found so far. In order to prove that statement, a statistical analysis had been done.

This paper begins with an overview of rational cubic Bézier, least-squares error and parameterization used based on centripetal method together with some basic concepts on data fitting. A gentle overview on the HS is also given. The G^1 continuity concept between two segments of our proposed data set is presented. Finally, method and its implementation, with some experimental results are presented. This method also had been compared with other two metaheuristic algorithms, which are genetic algorithm and particle swarm optimization on four different outline images. Statistical analysis also had been carried out in this paper to identify the reliability and effectiveness of this method.

2. Data fitting with rational cubic Bézier

A rational cubic Bézier function is defined as:

Let $\{(s_i, Q_i), i = 1, 2, \cdots, n\}$ be a given set of data point where $s_1 < s_2 < \cdots < s_n$. The piecewise rational cubic Bézier function is defined over each interval $I = [s_i, s_{i+1}]$, $i = 1, 2, \cdots, n-1$.

$$P(s) \equiv P(s_i) = \frac{(1-u)^3 C_0 + 3u(1-u)^2 w_1 C_1 + 3u^2(1-u) w_2 C_2 + u^3 C_3}{(1-u)^3 + 3u(1-u)^2 w_1 + 3u^2(1-u) w_2 + u^3} \tag{1}$$

where $u = \frac{s - s_i}{h_i}$ and $h_i = s_{i+1} - s_i, \quad u \in [0, 1]$.

w_1 and w_2 are shape parameters and $C_i, i = 0, 1, 2, 3$ are control points with C_0 and C_1 are fixed.

3. Least-squares error and reparameterization

By using centripetal method, the length of the data polygon can be written as

$$L = \sum_{i=1}^{n} |p_i - p_{i-1}|^{1/2} \tag{2}$$

Hence the parameters are

$$\left\{ s_0 = 0 \quad s_k = \frac{1}{L}\left(\sum_{i=1}^{k} |p_i - p_{i-1}|^{1/2} \right) \quad s_n = 1 \right\} \tag{3}$$

For a specified set of control points, the least-squares error function between $P(u_i)$ and $Q(s_i)$ is

$$E = \sum_{i=1}^{n} |P(u_i) - Q(s_i)|^2 \tag{4}$$

We are looking the values of w_1, w_2, C_1 and C_2 for which E is minimum.

4. Harmony search

Currently many phenomenon-mimicking meta-heuristic algorithms, such as genetic algorithm (GA), simulated annealing (SA), tabu search, ant colony optimization, and particle swarm optimization (PSO), have been used in various science and engineering problems. The advantages of these algorithms over calculus-based optimization algorithms include: not requiring complex gradient derivative and initial vector, ability to perform global search as well as local search, and efficiently handling discrete variables [5]. Harmony Search (HS) is a metaheuristic algorithm which was originally inspired by the improvisation process of Jazz musicians. The analogy between improvisation and optimization can be described as each musician corresponds to each decision variable; musical instrument's pitch range corresponds to decision variable's value range; musical harmony at certain time corresponds to solution vector at certain iteration; and audience's aesthetics corresponds to objective function [8]. Just like musical harmony is improved time after time, solution vector is improved iteration by iteration. HS imposes fewer mathematical requirements and does not require initial value settings of decisions variables. As the algorithm uses stochastic random searches, derivative information is also unnecessary. The steps in the procedure of harmony search are shown in Fig. 1. The basic steps are as follows [10]:

4.1. Initialize the problem and algorithm parameters

Suppose the optimization problem is specified as follows:

$$\text{Min } f(u) \quad \text{subject to} \quad u_i \in U, \quad i = 1, 2, \ldots, N \tag{5}$$

where $f(u)$ is an objective function, decision variables u_i, N is the number of decision variable, U is the set of the possible range of values for each decision variable, $Lu_i \leqslant U \leqslant Uu_i$ where Lu_i and Uu_i are lower and upper bounds for each decision variable, respectively. Parameters for HS are harmony memory size (HMS); harmony memory considering rate (HMCR); pitch adjusting rate (PAR); and number of improvisation (NI), or stopping criterion. The harmony memory (HM) is a memory location where all the solution vectors (sets of decision variables) are stored. At this step, HM is similar to the genetic pool in the GA where all of the data had been stored [10].

4.2. Initialize the harmony memory

HM matrix is filled with as many randomly generated solution vectors as the HMS

$$\mathrm{HM} = \begin{bmatrix} u_1^1 & u_2^1 & \cdots & u_{N-1}^1 & u_N^1 \\ u_1^2 & u_2^2 & \cdots & u_{N-1}^2 & u_N^2 \\ \vdots & \vdots & \vdots & \vdots & \vdots \\ u_1^{\mathrm{HMS}-1} & u_2^{\mathrm{HMS}-1} & \cdots & u_{N-1}^{\mathrm{HMS}-1} & u_N^{\mathrm{HMS}-1} \\ u_1^{\mathrm{HMS}} & u_2^{\mathrm{HMS}} & \cdots & u_{N-1}^{\mathrm{HMS}} & u_N^{\mathrm{HMS}} \end{bmatrix} \tag{6}$$

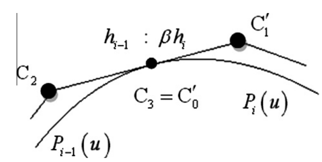

Figure 2 Geometric view of G^1 continuity.

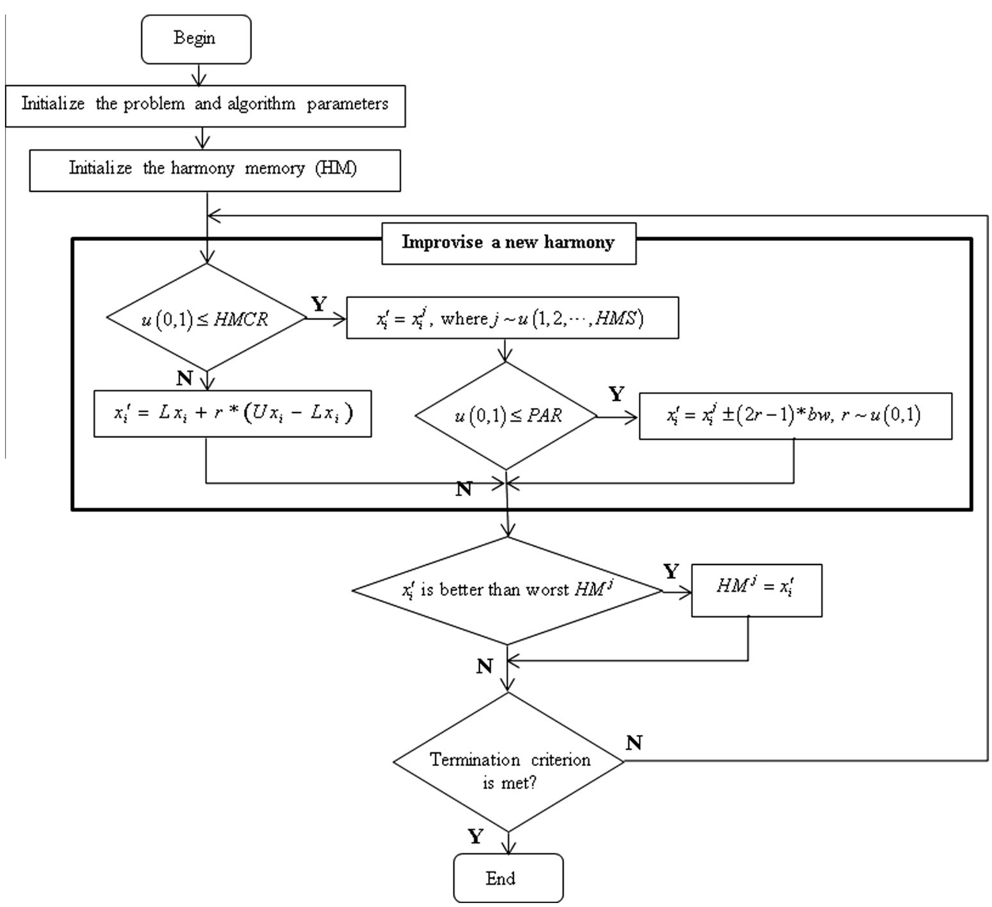

Figure 1 Procedure of harmony search algorithm.

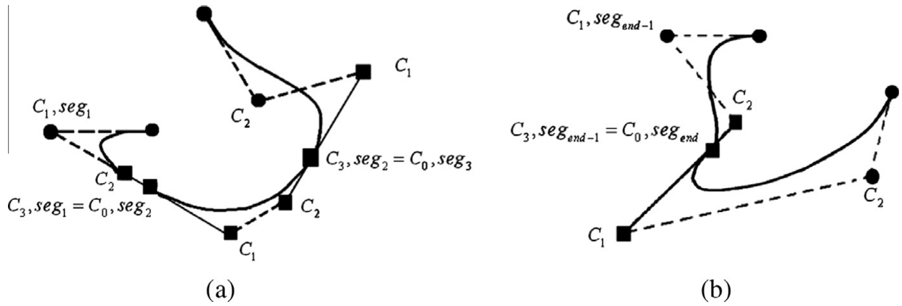

Figure 3 G^1 continuity illustration between (a) 3 segments and (b) 2 segments.

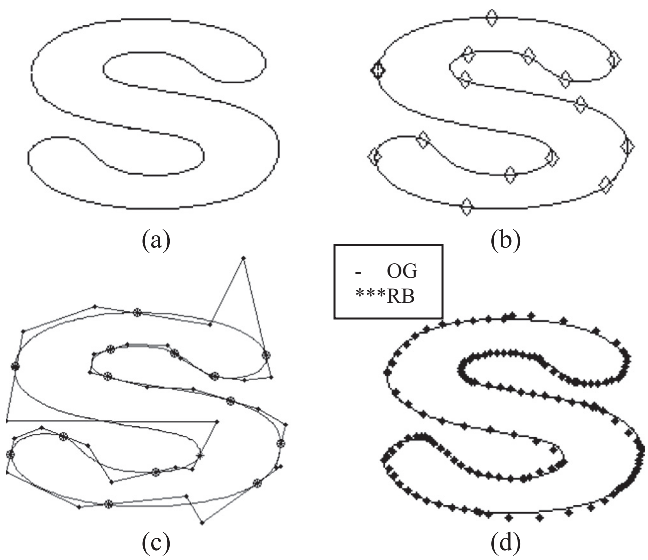

Figure 4 (a) Outline of the image, (b) outline with break points, (c) line connecting C_i's in every segment, (d) outline image with correspondent rational Bézier curve.

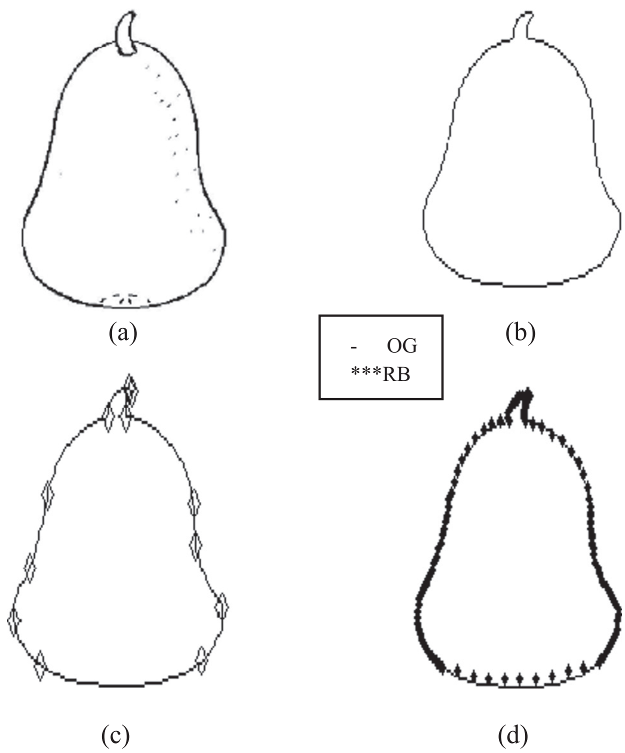

Figure 5 (a) Bitmapped image, (b) outline of the image, (c) outline with break points, (d) outline image with correspondent rational Bézier curve.

4.3. Improvise a new harmony

A new harmony vector, $u' = (u'_1, u'_2, \cdots, u'_N)$ is generated based on three rules: memory consideration, pitch adjustment and random selection. Generating a new harmony is called 'improvisation'. In the memory consideration, the value of the first decision variable, u'_1 for the new vector is chosen from any of the values in the specified HM range $(u_1'^1, u_1'^2, \cdots, u_1'^{\mathrm{HMS}})$, similar process to the other decision variables $(u'_2, u'_3, \cdots, u'_N)$. The detailed process of this steps is illustrated in Fig. 1.

4.4. Update harmony memory

If the new harmony vector, $u' = (u'_1, u'_2, \cdots, u'_N)$ is better than the worst harmony in the HM, judged in terms of the objective function value, the new harmony is included in the HM and the existing worst harmony is excluded from the HM.

4.5. Check

If the stopping criterion is satisfied, computation is terminated. Otherwise, steps 3 and 4 are repeated.

5. G^1 continuity between two segments

Marsh [11] gave a definition of geometric continuity by:

Suppose two regular curves $\mathbf{B}(s), s \in [s_0, s_1]$, and $\mathbf{C}(t)$, $t \in [t_0, t_1]$, meet at a point $\mathbf{P} = \mathbf{B}(s_1) = \mathbf{C}(t_0)$. Then the two curves said to meet with G^k – *continuity* whenever there is a Reparameterization $\beta : [u_0, u_1] \to [s_0, s_1]$ such that $s_1 = \beta(u_1)$ and

$$\frac{d^i\mathbf{B}}{du^i}(\beta(u))|_{u=u_1} \quad \frac{d^i\mathbf{C}}{dt^i}(t)|_{t=t_0} \tag{7}$$

for all $i = 0, \cdots, k$. This type of continuity is called *geometric continuity*.

In a geometric view, for a regular curve $P(u)$, G^1 at u if it is G^0 continuous and it possesses continuous unit tangent vector,

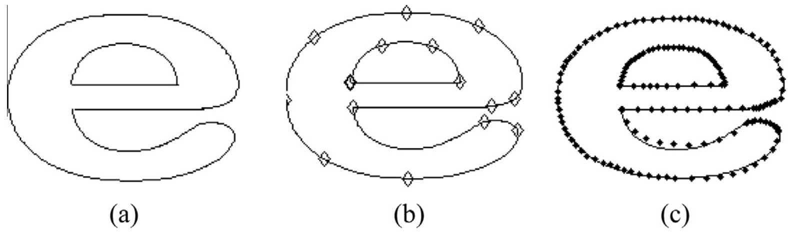

Figure 6 (a) Outline of the image, (b) outline with break points, (c) outline image with correspondent rational Bézier curve.

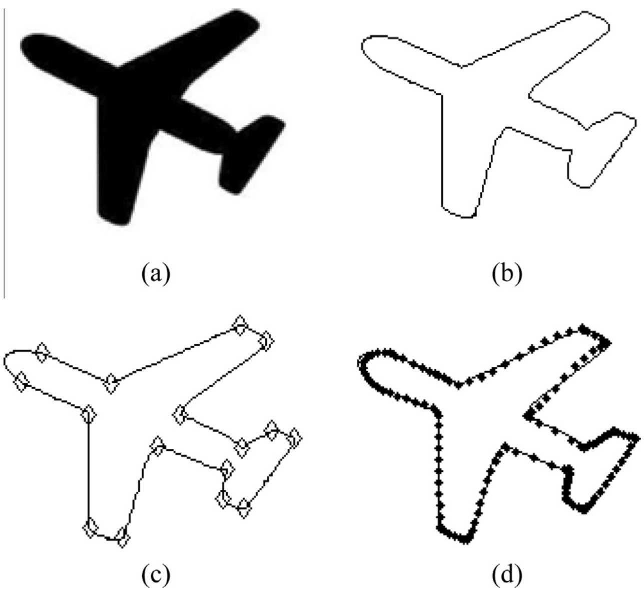

Figure 7 (a) Bitmapped image, (b) outline of the image, (c) outline with break points, (d) outline image with correspondent rational Bézier curve.

$$\beta P'(u^-) = P'(u^+) \tag{8}$$

where $\beta = \frac{\|P'(u^+)\|}{\|P'(u^-)\|} > 0$

$P'(u^-)$ and $P'(u^+)$ point to the same direction with different values of magnitude as in Fig. 2.

Bézier points C_2, C_3 and C'_1 must be collinear but the ratio of $\|C_2C_3\|$ and $\|C'_0C'_1\|$ are not fixed, where β is utilized to break the chain.

6. Method and implementation

In order to implement HS, Eq. (4) is used as the objective function. HS parameters in this work are HM = 5, HMCR = 0.9, PAR = 0.3 and bw = 0.03. All these values of parameters are the usual choice in HS community and also supported based on empirical results by [13]. According to results by Omran and Mahdavi [13], in general, using a small HM seems to be a good and logical choice with the added advantage of reducing space requirements. Actually, since HM resembles the short-term memory of a musician which is known to be small, it is logical to use a small HM as in the paper used the smallest value of HM is 5. As for HMCR, a large value for HMCR (e.g. 0.95) generally improves the performance of the HS. The experiments show that using a relatively small constant value for PAR seems to improve the performance of the HS.

As the beginning, all the data extracted from the outline boundary of the images had been broke into a few curve segments. The completion of the procedures to fit all the data consists of 3 sections: original segments, segment between two segments and end segment.

Table 1 G^1 continuity analysis.

nth joint	Fig. 5		Fig. 6		Fig. 7		Fig. 8	
	β_x	β_y	β_x	β_y	β_x	β_y	β_x	β_y
1	4.26051098	4.26051098	0.01893534	0.01893534	10.43118780	10.43118780	0.59910652	0.59910652
2	0.16440373	0.16440373	0.04707052	0.04707052	0.38101031	0.38101039	1.72965880	1.72965880
3	−2.77452417	−2.77452417	3.30416527	3.30416527	4.32293758	4.32293758	5.19218689	5.19218689
4	−0.34379848	−0.34379848	0.41811991	0.41811991	2.05956026	2.05956026	1.32544346	1.32544346
5	1.01815645	1.01815645	1.53058122	1.53058122	1.81849452	1.81849452	0.92138456	0.92138456
6	0.01585093	0.01585093	0.37198273	0.37198273	0.88708711	0.88708711	0.65161496	0.65161496
7	2.55695847	2.55695847	4.12417886	4.12417886	1.17072419	1.17072419	1.08933812	1.08933812
8	0.49683132	0.49683132	−2.63191694	0.65945804	0.42307881	0.42307881	1.06743386	1.06743386
9	−0.34326318	−0.91623243	0.43726459	0.43726459	7.93291619	7.93291619	0.39554224	0.39554224
10	0.30432804	0.30432804	0.409990409	0.40999041	0.20215543	0.20215543	0.84602743	0.84602743
11	3.74608222	3.74608222	−3.87751453	6.62429858	1.23469281	1.23469281	1.66866911	1.66866911
12	−1.50717641	0.18755597	–	–	1.78335501	1.78335501	0.87416563	0.87416563
13	−2.00241487	4.31008604	–	–	–	–	3.24574994	3.24574994
14	1.04244158	1.04244158	–	–	–	–	0.35296832	0.35296832
15	1.73650617	1.73650617	–	–	–	–	–	–

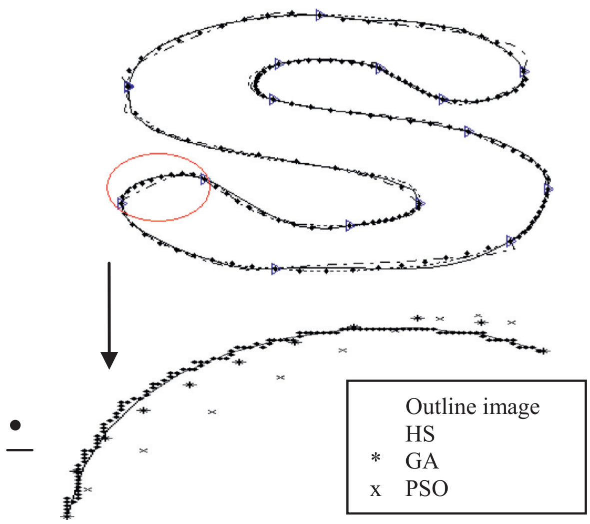

Figure 8 Data fitting for outline for alphabet ‘S’ with 2593 data points. The highlight segment consists of 113 data points, HS error = 0.0008, GA error = 0.0025 and PSO error = 0.0803.

6.1. Original segments

In this section, only the odd segments (1,3,...) will be considered and all the data in the segment will be approximated without any constraints. The size of w_1 and w_2 is in $[0, 2]$. The search space for C_1 and C_2 are estimated as follows:

Let a segment consists a set of points $(d_1, d_2, \cdots, d_{end}) \in \mathbb{R}^2$ while C_1^* and C_2^* are extremum points in the segments. The size of each C_1^* and C_2^* is determined by:

$$\text{size of } C_i^* = |d_{\max} - d_{\min}|, \quad i = 1, 2 \tag{9}$$

6.2. Segment between two segments

For this section, the even segments (2,4,...) will be considered and all the data in the segment will be approximated with certain constraints, which are as follows:

Suppose a set of data has three segments, seg_1, seg_2 and seg_3 as in Fig. 3(a), each segment of rational cubic Bézier curve

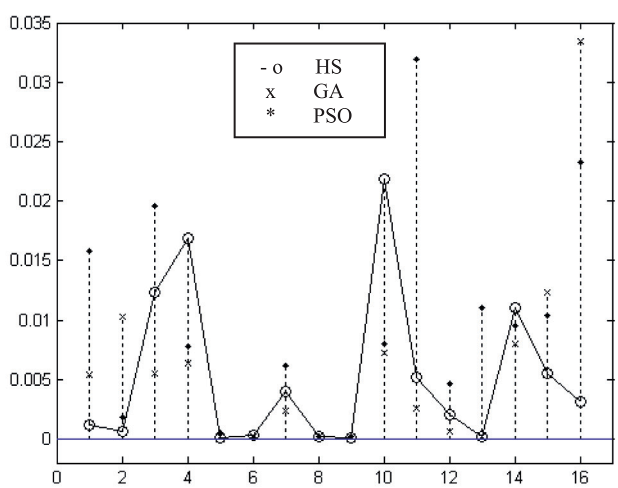

(a) Aeroplane (1875 data points)

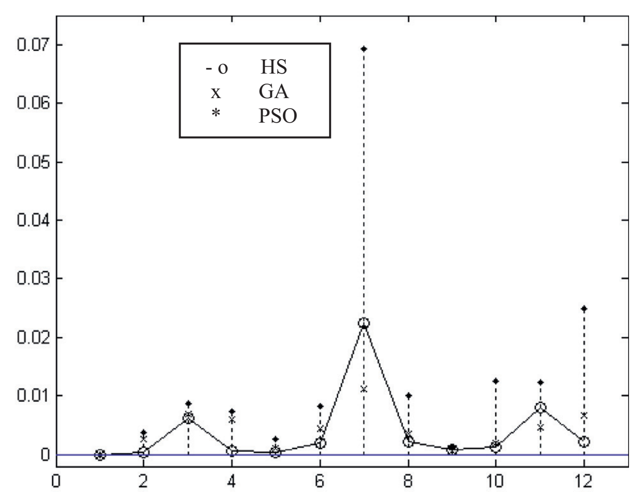

(b) Pear (1433 data points)

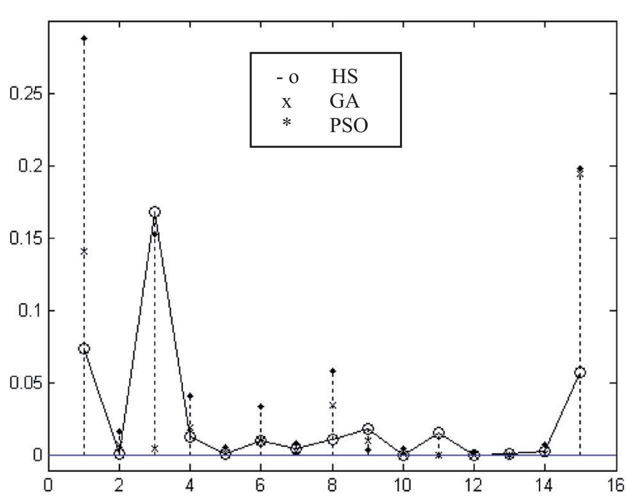

(c) Letter ‘e’ (2783 data points)

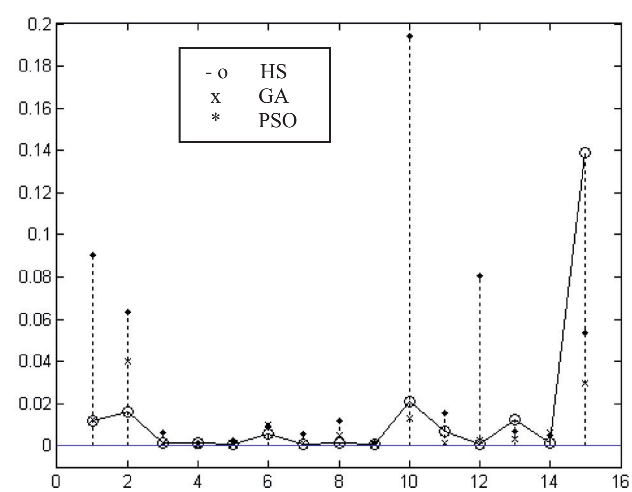

(d) Letter ‘s’ (2593 data points)

Figure 9 Minimum least-squares error for each segment of test outline images.

Table 2 Descriptive data of four outline images.

	Best	Worst	Mean	Median	Variance	Standard deviation
Letter 's'						
HS	0.0500	0.1400	0.1087	0.1063	0.00099	0.03153
GA	0.0900	0.1700	0.1599	0.1533	0.00172	0.04151
PSO	0.2300	0.7300	0.5610	0.5377	0.03745	0.19353
Letter 'e'						
HS	0.1151	0.2567	0.1648	0.1633	0.00129	0.03597
GA	0.1837	0.9036	0.6007	0.5963	0.03636	0.19068
PSO	0.7127	1.1592	0.9362	0.9595	0.01072	0.10354
Aeroplane						
HS	0.0437	0.0890	0.068247	0.06665	0.00013	0.01161
GA	0.0290	0.1393	0.074257	0.0712	0.00047	0.02162
PSO	0.1082	0.3716	0.22588	0.22215	0.00241	0.04910
Pear						
HS	0.0123	0.0222	0.01695	0.0168	0.00000	0.00274
GA	0.0235	0.0426	0.03226	0.0321	0.00003	0.00512
PSO	0.1107	0.2482	0.174553	0.1728	0.00179	0.04227

Table 3 Tests of normality.

	Kolmogorov–Smirnov			Shapiro–Wilk		
	Statistic	df	Sig.	Statistic	df	Sig.
Letter 's'_HS	0.087	30	0.200	0.960	30	**0.308**
Letter 's'_GA	0.108	30	0.200	0.971	30	**0.572**
Letter 's'_PSO	0.169	30	0.029	0.943	30	**0.109**
Letter 'e'_HS	0.101	30	0.200	0.947	30	**0.138**
Letter 'e'_GA	0.172	30	0.024	0.932	30	**0.056**
Letter 'e'_PSO	0.183	30	0.012	0.935	30	**0.067**
Aeroplane_HS	0.073	30	0.200	0.980	30	**0.825**
Aeroplane_GA	0.102	30	0.200	0.962	30	**0.345**
Aeroplane_PSO	0.112	30	0.200	0.953	30	**0.204**
Pear_HS	0.172	30	0.024	0.938	30	**0.079**
Pear_GA	0.102	30	0.200	0.973	30	**0.621**
Pear_PSO	0.088	30	0.200	0.948	30	**0.153**

should consist of (C_0, C_1, C_2, C_3), the control points. All these three segments are G^1. Therefore, data fitting in seg_2 must fulfil certain constraints involving seg_1 and seg_3.

The size of w_1 and w_2 is in $[0, 2.5]$. While search space for C_1^* and C_2^* are similar to the previous section but one of the variables, $C_i = (x_i, y_i)$ depends on the other one, for which $[(C_2, seg_i), (C_3, seg_i = C_0, seg_{i+1}), (C_1, seg_{i+1})], \quad i = 1, 2$ must be collinear. For this section, the number of decision variables for HS is reduced.

6.3. End segments

The end segment, seg_{end} will be considered if total data points are even. All the data in the segment will be approximated with certain constraints, which are:

Table 4 Independent group ANOVA.

ANOVA						
Source of variation	SS	df	MS	F	P-value	F crit
(a) Letter 's'						
Between Groups	3.681533865	2	1.840767	137.4745378	**1.16929E−27**	3.101296
Within Groups	1.16491916	87	0.01339			
Total	4.846453025	89				
(b) Letter 's'						
Between Groups	8.974284755	2	4.487142	278.2765	**1.56918E−38**	3.101295757
Within Groups	1.402854501	87	0.016125			
Total	10.37713926	89				
(c) Aeroplane						
Between Groups	0.47874	2	0.23937	238.294	**5.03791E−36**	3.101295757
Within Groups	0.087393	87	0.001005			
Total	0.566133	89				
(d) Pear						
Between Groups	0.453205995	2	0.226603	373.463	**1.99546E−43**	3.101296
Within Groups	0.052788262	87	0.000607			
Total	0.505994257	89				

Table 5 *F*-test of two samples for variances.

F-test two-sample for variances			*F*-test two-sample for variances			*F*-test two-sample for variances		
	GA	*HS*		*PSO*	*HS*		*PSO*	*GA*
(a) Letter 's'								
Mean	0.159926667	0.10868	Mean	0.561043333	0.10868	Mean	0.561043333	0.1599267
Variance	0.001723099	0.000994	Variance	0.037452536	0.000994	Variance	0.037452536	0.0017231
Observations	30	30	Observations	30	30	Observations	30	30
df	29	29	df	29	29	Df	29	29
F	1.733516623		*F*	37.67896352		*F*	21.73556516	
$P(F<=f)$ one-tail	**0.072201294**		$P(F<=f)$ one-tail	**2.71646E−16**		$P(F<=f)$ one-tail	**4.75936E−13**	
F critical one-tail	1.619899621		*F* critical one-tail	1.860811435		*F* critical one-tail	1.860811435	
F-test two-sample for variances			*F*-test two-sample for variances			*F*-test two-sample for variances		
	HS	*GA*		*HS*	*PSO*		*GA*	*PSO*
(b) Letter 'e'								
Mean	0.164833333	0.6007	Mean	0.164833333	0.936147	Mean	0.6007	0.936147
Variance	0.001293492	0.03636	Variance	0.001293492	0.010721	Variance	0.036359512	0.010721
Observations	30	30	Observations	30	30	Observations	30	30
df	29	29	df	29	29	df	29	29
F	0.035575064		*F*	0.120647051		*F*	3.391337565	
$P(F<=f)$ one-tail	**1.4988E−14**		$P(F<=f)$ one-tail	**8.71309E−08**		$P(F<=f)$ one-tail	**0.000769416**	
F critical one-tail	0.537399965		*F* critical one-tail	0.537399965		*F* critical one-tail	1.860811435	
F-test two-sample for variances			*F*-test two-sample for variances			*F*-test two-sample for variances		
	HS	*GA*		*HS*	*PSO*		*GA*	*PSO*
(c) Aeroplane								
Mean	0.068247	0.074257	Mean	0.068246667	0.22588	Mean	0.074256667	0.22588
Variance	0.000135	0.000468	Variance	0.000134765	0.002411209	Variance	0.000467574	0.002411
Observations	30	30	Observations	30	30	Observations	30	30
df	29	29	df	29	29	Df	29	29
F	0.288223		F	0.055891197		F	0.193916687	
$P(F<=f)$ one-tail	**0.000634**		$P(F<=f)$ one-tail	**6.20171E−12**		$P(F<=f)$ one-tail	**1.54586E−05**	
F critical one-tail	0.412637		*F* critical one-tail	0.412636754		*F* critical one-tail	0.412636754	
F-test two-sample for variances			*F*-test two-sample for variances			*F*-test two-sample for variances		
	HS	*GA*		*HS*	*PSO*		*GA*	*PSO*
(d) Pear								
Mean	0.01695	0.03226	Mean	0.01695	0.174553	Mean	0.03226	0.174553333
Variance	7.51776E−06	2.62E−05	Variance	7.51776E−06	0.001787	Variance	2.62E−05	0.001786553
Observations	30	30	Observations	30	30	Observations	30	30
df	29	29	df	29	29	Df	29	29
F	0.286781845		*F*	0.004207969		*F*	0.014673	
$P(F<=f)$ one-tail	**0.000607464**		$P(F<=f)$ one-tail	0		$P(F<=f)$ one-tail	0	
F critical one-tail	0.412636754		*F* critical one-tail	0.412636754		*F* critical one-tail	0.412637	

Suppose a set of data has two last segments, $seg_{\text{end}-1}, seg_{\text{end}}$ as in Fig. 3(b). All these two segments should have smooth joints with G^1 continuity. Therefore, data fitting in seg_{end} must fulfil certain constraints involving $seg_{\text{end}-1}$.

The size of w_1 and w_2 is in $[0, 2.5]$. While search space for C_1 and C_2 are similar to the previous section but one of the variable, $C_i = (x_i, y_i)$ depends on the other one at the last joint, i.e., $[(C_2, seg_{\text{end}-1}), (C_3, seg_{\text{end}-1} = C_0, seg_{\text{end}}), (C_1, seg_{\text{end}})]$ must be collinear.

7. Demonstration and experimental results

Proposed data fitting method has been implemented practically in Figs. 4–7(a). Each data segments are evaluated at uniformly distributed values of u in its domain to generate a collection of 201 data points on the interval of $[0, 1]$.

Figs. 4(d), 5(d), 6(c) and 7(d) are the best fitting curves, where OG is the original graph and, RB is the corresponding rational Bézier curve. Fig. 4(c) shows lines which connects

Table 6 *T*-test of two samples assuming unequal variances.

t-test: two-sample assuming unequal variances			*t*-test: two-sample assuming unequal variances			*t*-test: two-sample assuming unequal variances		
	HS	*GA*		*HS*	*PSO*		*GA*	*PSO*
(a) Letter 's'								
Mean	0.10868	0.159927	Mean	0.10868	0.561043	Mean	0.159926667	0.5610433
Variance	0.000993991	0.001723	Variance	0.000993991	0.037453	Variance	0.001723099	0.0374525
Observations	30	30	Observations	30	30	Observations	30	30
Hypothesized mean difference	0		Hypothesized mean difference	0		Hypothesized mean difference	0	
df	54		df	31		df	32	
t stat	−5.38485789		*t* stat	−12.6362865		*t* stat	−11.1000084	
$P(T<=t)$ one-tail	**8.08374E−07**		$P(T<=t)$ one-tail	**4.56312E−14**		$P(T<=t)$ one-tail	**8.30798E−13**	
t critical one-tail	2.397409645		*t* critical one-tail	2.452824193		*t* critical one-tail	2.448677634	
$P(T<=t)$ two-tail	1.61675E−06		$P(T<=t)$ two-tail	9.12624E−14		$P(T<=t)$ two-tail	1.6616E−12	
t critical two-tail	2.669984796		*t* critical two-tail	2.744041919		*t* critical two-tail	2.738481482	

t-test: two-sample assuming unequal variances			*t*-test: two-sample assuming unequal variances			*t*-test: two-sample assuming unequal variances		
	HS	*GA*		*HS*	*PSO*		*GA*	*PSO*
(b) Letter 'e'								
Mean	0.164833333	0.6007	Mean	0.164833333	0.936147	Mean	0.6007	0.936147
Variance	0.001293492	0.03636	Variance	0.001293492	0.010721	Variance	0.036359512	0.010721
Observations	30	30	Observations	30	30	Observations	30	30
Hypothesized mean difference	0		Hypothesized mean difference	0		Hypothesized mean difference	0	
Df	31		df	36		df	45	
t stat	−12.3030977		*t* stat	−38.5419363		*t* stat	−8.4676361	
$P(T<=t)$ one-tail	**9.14105E−14**		$P(T<=t)$ one-tail	**3.6084E−31**		$P(T<=t)$ one-tail	**3.63208E−11**	
t critical one-tail	1.695518783		*t* critical one-tail	1.688297714		*t* critical one-tail	1.679427393	
$P(T<=t)$ two-tail	1.82821E−13		$P(T<=t)$ two-tail	7.2168E−31		$P(T<=t)$ two-tail	7.26417E−11	
t critical two-tail	2.039513446		*t* critical two-tail	2.028094001		*t* critical two-tail	2.014103389	

t-test: two-sample assuming unequal variances			*t*-test: two-sample assuming unequal variances			*t*-test: two-sample assuming unequal variances		
	HS	*GA*		*HS*	*PSO*		*GA*	*PSO*
(c) Aeroplane								
Mean	0.068247	0.074257	Mean	0.068246667	0.22588	Mean	0.074256667	0.22588
Variance	0.000135	0.000468	Variance	0.000134765	0.002411	Variance	0.000467574	0.002411
Observations	30	30	Observations	30	30	Observations	30	30
Hypothesized mean difference	0		Hypothesized mean difference	0		Hypothesized mean difference	0	
df	44		df	32		df	40	
t stat	−1.34127		*t* stat	−17.1112491		*t* stat	−15.4782647	
$P(T<=t)$ one-tail	**0.093358**		$P(T<=t)$ one-tail	**5.79073E−18**		$P(T<=t)$ one-tail	**8.71294E−19**	
t critical one-tail	1.30109		*t* critical one-tail	1.308572793		*t* critical one-tail	1.303077053	
$P(T<=t)$ two-tail	0.186717		$P(T<=t)$ two-tail	1.15815E−17		$P(T<=t)$ two-tail	1.74259E−18	
t critical two-tail	1.68023		*t* critical two-tail	1.693888748		*t* critical two-tail	1.683851013	

t-test: two-sample assuming unequal variances			*t*-test: two-sample assuming unequal variances			*t*-test: two-sample assuming unequal variances		
	HS	*GA*		*HS*	*PSO*		*GA*	*PSO*
(d) Pear								
Mean	0.01695	0.03226	Mean	0.01695	0.174553	Mean	0.03226	0.174553
Variance	7.51776E−06	2.62E−05	Variance	7.51776E−06	0.001787	Variance	2.62142E−05	0.001787
Observations	30	30	Observations	30	30	Observations	30	30
Hypothesized	0		Hypothesized	0		Hypothesized	0	

(*continued on next page*)

Table 6 (*continued*)

t-test: two-sample assuming unequal variances			*t*-test: two-sample assuming unequal variances			*t*-test: two-sample assuming unequal variances		
	HS	*GA*		*HS*	*PSO*		*GA*	*PSO*
mean difference			mean difference			mean difference		
df	44		df	29		df	30	
t stat	−14.4382645		*t* stat	−20.3800972		*t* stat	−18.3051871	
$P(T<=t)$ one-tail	**1.33021E−18**		$P(T<=t)$ one-tail	**4.92526E−19**		$P(T<=t)$ one-tail	**3.95498E−18**	
t critical one-tail	2.414134368		*t* critical one-tail	2.46202136		*t* critical one-tail	2.457261542	
$P(T<=t)$ two-tail	2.66042E−18		$P(T<=t)$ two-tail	9.85052E−19		$P(T<=t)$ two-tail	7.90995E−18	
t critical two-tail	2.692278266		*t* critical two-tail	2.756385904		*t* critical two-tail	2.749995654	

all the C_i's in every segment which applies G^1 continuity between two segments.

Table 1 summarizes the G^1 continuity analysis for above test outline images. Values of β for each test function are calculated based on Eq. (8).

7.1. Comparison with other methods and analysis

Our G^1 HS approach performs well for the above test outline images. To support this claim, a comparison with recent alternative curve fitting based on soft computing techniques has been carried out. There were a few of soft computing method used in this data fitting problem, such as curve fitting by B-splines using GA by Gálvez et al. [4], Sarfraz [19] used cubic spline by SA and Yahya [15–16] proposed an approach of curve fitting by PSO. Here a comparison between HS, GA and PSO that used on the similar data points. The procedure of PSO was taken from [2]. Fig. 8 highlights on a segment of letter 's' and shows that HS approach better the data points within the same time range as others. Fig. 9 summarizes the least-squares errors of each segment for test outline images and in the graphs; the output for HS in segments 4 and 10 for the first image, segment 3 in third image and also segment 15 in fourth image are larger than others as there are cusps before the segments. However, HS approach each outlines better by looking at the total of least-squares error in the data sets.

7.2. Statistical analysis

All evolutionary algorithms, including HS, GA and PSO are stochastic population based search methods. Accordingly, there is no guarantee that the optimal solution will be reached consistently. Therefore, in order to deny that there is a guarantee that HS can be used to have better approximation to the global optimal solution, a comparison on optimization problem using such algorithm where a statistical analysis had been carried out. 30 sample data of total least-squares error of four outlines for methods HS, GA and PSO were being used with the time taken for all the data which were fixed.

From Table 2, it is clearly shows the prominent method for all images based on descriptive data is HS. All the sample data had been assessed their normality by the Shapiro-Wilks statistics in order to verify their significance different between their variance. The results of normality were shown in Table 3.

According to Table 4, there is sufficient evidence that the HS has the smallest variation compared to GA and PSO at 1–10% significance level (p-value: 0.0722, 2.7164×10^{-16}; 1.4988×10^{-14}, 8.7131×10^{-8}; 0.0006, 6.2017×10^{-12}; 0.0006, 0.0000). While Table 5 shows that the mean of HS is the smallest value compared to GA and PSO at 1–10% significance level (p-value: 8.0837×10^{-7}, 4.5621×10^{-14}; 9.1411×10^{-14}, 3.6084×10^{-31}; 0.0934, 5.7907×10^{-18}; 1.3302×10^{-18}, 4.9253×10^{-19}). While, Table 6 also supported the same conclusion of HS compared to other two methods. These leads to say that, in this study, HS was found to give the best fit for data fitting using rational cubic Bezier for each segment of all tested outlines images. These results give strong indication that the HS method is more stable and accurate compared to GA and PSO.

8. Conclusions

A derivative-free real parameter optimization technique, based on HS, is implemented for data fitting. This technique optimizes the control points and shape parameters of rational cubic Bézier curves in order to approximate the data sets. The technique data fitting by G^1 continuity for every joint of segments for the whole data set, the rational Bézier ultimately produces optimal results in approximating the data. It provides an optimal fit with an efficient computation cost. A comparison between HS, GA and PSO were done on four different outline images and a few of statistical testing also had been carried out over a 30 sample data set each. Based on the statistical analysis carried out on the sample data, there are sufficient evidences to say that HS gave a smaller values of error compared to other two methods.

References

[1] Cai HJ, Wang GJ. Constrained approximation of rational Bézier curves based on a matrix expression of its end points continuity condition. Comput Aided Des 2010;42(6):495–504.

[2] Das S, Abraham A, Konar A. Particle swarm optimization and differential evolution algorithms: technical analysis, applications and hybridization perspectives. Stud Comput Intel (SCI) 2008;116:1–38.

[3] Gálvez A, Iglesias A. Efficient particle swarm optimization approach for data fitting with free knot –splines. Comput Aided Des 2011;43(12):1683–92.

[4] Gálvez A, Iglesias A, Puig-Pey J. Iterative two-step genetic-algorithm-based method for efficient polynomial B-spline surface reconstruction. Inf Sci 2012;182:56–76.

[5] Geem ZW, Sim K-B. Parameter-setting-free harmony search algorithm. Appl Math Comput 2010;217:3881–9.

[6] Huang W-X, Jin C-J, Wang G-J. Approximate Bézier curves by cubic LN curves. Appl Math Comput 2011;218:3083–92.

[7] Hur S, Kim T. Finding the best conic approximation to the convolution curve of two compatible conics based on Hausdorff distance. Comput Aided Des 2009;41(7):513–24.

[8] Lee KS, Geem ZW. A new meta-heuristic algorithm for continuous engineering optimization: harmony search theory and practice. Comput Methods Appl Mech Eng 2005;194:3902–33.

[9] Lu L. Sample-based polynomial approximation of rational Bézier curves. J Comput Appl Math 2011;235(6):1557–63.

[10] Mahdavi M, Fesanghary M, Damangir E. An improved harmony search algorithm for solving optimization problems. Appl Math Comput 2007;188(2):1567–79.

[11] Marsh D. Applied geometry for computer graphics and CAD. 2nd ed. London: Springer-Verlag; 2005.

[12] Mortenson ME. Geometric modeling. Canada: John Wiley & Sons; 1997.

[13] Omran MGH, Mahdavi M. Global-best harmony search. Appl Math Comput 2008;198:643–56.

[14] Yahya F, Ali JM, Majid AA, Ibrahim A. An automatic generation of G1 curve fitting of arabic characters. In: International conference on computer graphics imaging and visualisation CGIV06; 2006. p. 1–6.

[15] Yahya ZR, M Piah AR, Majid AA. G1 continuity conics for curve fitting using particle swarm optimization. In: 2011 15th international conference on information visualisation; 2011. p. 497–501.

[16] Yahya ZR, Piah ARM, Majid AA. Curve fitting conic by evolutionary computing. J Math Stat 2012;8(1):107–10.

[17] Shen L-Y, Yuan C-M, Gao X-S. Certified approximate of parametric space curves with cubic B-spline curves. Comput Aided Des 2012;29:643–63.

[18] Sarfraz M. Vectorizing outlines of generics shapes by cubic spline using simulated annealing. Int J Comp Math 2010;87(8):1736–51.

[19] Sarfraz M. Intelligent approaches for vectorizing image outlines. J Software Eng Appl 2012;5:78–83.

[20] Stamati V, Fudos I. On reconstructing 3D feature boundaries. Comput-Aid Des Appl 2008;5(1–4):316–24.

[21] Yang Y-J, Zeng W, Yang C-L, Meng X-X, Yong J-H, Deng B. G^1 continuous approximate curves on NURBS surfaces. Comput Aided Des 2012;44:824–34.